Evidence for a Mixed-Ligand [4Fe-4S] Cluster in the C14D Mutant of PsaC. Altered Reduction Potentials and EPR Spectral Properties of the F_A and F_B Clusters on Rebinding to the P700-F_X Core†

Lian Yu,‡ Donald A. Bryant,§ and John H. Golbeck*,‡

Department of Biochemistry and Center for Biological Chemistry, University of Nebraska, Lincoln, Nebraska 68588-0664, and Department of Biochemistry and Molecular Biology and Center for Biomolecular Structure and Function, The Pennsylvania State University, University Park, Pennsylvania 16802

Received November 29, 1994; Revised Manuscript Received April 11, 1995⊗

ABSTRACT: PsaC-C14D (cysteine 14 replaced by aspartic acid) contains a [3Fe-4S] and a [4Fe-4S] cluster in the F_B and F_A sites of the free protein [Yu, L., Zhao, J., Lu, W., Bryant, D. A., & Golbeck, J. H. (1993) *Biochemistry 32*, 8251−8258]. When PsaC-C14D is rebound to a photosystem I (PS I) core, the *g*-values of 2.043, 1.939, and 1.853 appear similar to F_A in a wild-type PS I complex [Zhao, J. D., Li, N., Warren, P. V., Golbeck, J. H., & Bryant, D. A. (1992) *Biochemistry 31*, 5093−5099]. The reconstituted PsaC-C14D−PS I complex does not contain a [3Fe-4S] cluster; rather, a set of resonances with a rhombic line shape, a g_{av} of ~1.97, and broad line widths indicate the presence of a mixed-ligand [4Fe-4S] cluster, termed F_B', in the aspartate site. Both F_A and F_B' become photoreduced at 15 K, and show an interaction spectrum when reduced within the same reaction center. An electrochemical redox study shows that F_A and F_B' titrate with midpoint potentials near −600 mV at pH 10.0. Single-turnover flash experiments indicate that F_A and F_B' function as efficient electron acceptors at room temperature, and $NADP^+$ photoreduction rates are about 70% that of a reconstituted PsaC−PS I complex. A population of $S = {}^3/_2$, [4Fe-4S] clusters was tentatively identified in the free PsaC-C14D protein by characteristic EPR resonances in the $g = 5.3$ region. It is proposed that P700-F_X cores have a high affinity for PsaC-C14D that contains two cubane clusters, and that on rebinding, the mixed-ligand cluster in the F_B' site crosses over from the $S = {}^3/_2$ to the $S = {}^1/_2$ spin state. These results show that electron throughput from F_X to ferredoxin in the PsaC-C14D−PS I complex remains efficient even though the spectroscopic and thermodynamic properties of F_A and F_B' are altered by the presence of the mixed-ligand iron−sulfur cluster in the F_B site.

Iron−sulfur clusters play an essential role in electron transfer processes in the energy transducing membranes of photosynthesis and respiration. In photosystem I (PS I),[1] two [4Fe-4S] clusters, F_A and F_B, participate in transferring an electron from F_X, an interpolypeptide [4Fe-4S] cluster, to either ferredoxin or flavodoxin. Crystals of the detergent-isolated PS I complex from *Synecococcus* sp. diffract to a resolution of 4 Å (Fromme et al., 1994), and a structural model based upon the electron density map at a resolution of 6 Å has been published (Krauss et al., 1993). The crystal structure depicts the three iron−sulfur clusters forming an irregular triangle with one cluster 15 Å and the other 22 Å from the F_X cluster that lies on a pseudo-C_2 axis of symmetry (and roughly on the membrane surface). Although the distances and bond angles are resolved, the crystal structure model provides no information on which of these two clusters represents F_A and F_B, and no information on whether one or both clusters function in forward electron transfer to ferredoxin and flavodoxin.

One approach to address these issues is to employ directed mutagenesis combined with biochemical resolution and reconstitution protocols to render F_A and F_B kinetically or thermodynamically distinct. The factors that control the redox potentials of iron−sulfur clusters are not well understood; in soluble ferredoxins, the potentials are thought to be modulated in part by access of solvent water to the local environment of the cluster (Langen et al., 1992; Jensen et al., 1994). Our strategy for studying membrane-bound iron−sulfur proteins is to alter the electronic structure of the clusters by changing the ligands to one of the cubane irons. Recent studies have shown that the incorporation of aspartic acid into positions 14 and 51 of PsaC leads to the incorporation of [3Fe-4S] clusters into the modified sites and [4Fe-4S] clusters in the unmodified sites of the free proteins (Yu et al., 1993). The reduction potentials of the [3Fe-4S] clusters were measured to be −100 mV, a value nearly 400−450 mV more oxidizing than F_A or F_B in the wild-type protein. When the PsaC-C14D and PsaC-C51D were rebound to a P700-F_X core in the presence of PsaD, the *g*-values and line shapes of the [4Fe-4S] clusters were identical to F_A and F_B in the wild-type PS I complexes (Zhao

† Published as Journal Series No. 10952 of the University of Nebraska Agricultural Research Division. Supported by grants from the National Science Foundation (MCB-9205756 to J.H.G. and MCB-9206851 to D.A.B.).

* Address correspondence to this author. Telephone: (402) 472-2931. Fax: (402) 472-7842.

‡ University of Nebraska.

§ The Pennsylvania State University.

⊗ Abstract published in *Advance ACS Abstracts,* June 1, 1995.

[1] Abbreviations: PsaC-C14D, mutant PsaC protein in which cysteine 14 has been replaced by aspartic acid; PsaC-C51D, mutant PsaC protein in which cysteine 51 has been replaced by aspartic acid; Chl, chlorophyll; DCPIP, dichlorophenolindophenol; DTT, dithiothreitol; EGTA, [ethylenebis(oxyethylenenitrilo)]tetraacetic acid; EPR, electron paramagnetic resonance; IPTG, isopropyl β-D-thiogalactopyranoside; PMS, phenazine methosulfate; MES, 2-(*N*-morpholino)ethanesulfonic acid; PS I, photosystem I; β-ME, β-mercaptoethanol; Tris, tris-(hydroxymethyl)aminomethane.

0006-2960/95/0434-7861$09.00/0

et al., 1992). The [4Fe-4S] cluster in PsaC-C51D−PS I assumed g-values of 2.063, 1.934, and 1.879, which identified that center as F_B; the [4Fe-4S] cluster in PsaC-C14D−PS I assumed g-values of 2.043, 1.942, and 1.853, which identified that center as F_A. Assuming a pattern of cysteine ligation analogous to that of other 2[4Fe-4S] ferredoxins such as that of *Peptococcus aerogenes,* the cysteines which provide ligands to the F_A and F_B clusters were deduced (Zhao et al., 1992).

The EPR signals characteristic of the [3Fe-4S] cluster observed in the free PsaC-C14D protein were not observed in the reconstituted PsaC-C14D−PS I complex. Instead, a complex set of resonances were seen around $g = 2$ when the sample was frozen in darkness. These resonances were not enhanced or diminished on subsequent illumination at 15 K or at 298 K. In this paper, the results of a comprehensive search are reported for the [3Fe-4S] clusters in PsaC-C14D−PS I. Although the "missing" [3Fe-4S] clusters were not found, a new spin system was uncovered that has characteristics of a mixed-ligand, [4Fe-4S] cluster in the F_B site. This newly-identified cluster showed photochemical behavior, spin relaxation properties, and a reduction potential distinct from those of F_B in a wild-type PS I complex.

MATERIALS AND METHODS

Biochemical Protocols. The P700-F_X core from *Synechococcus* sp. strain PCC 6301 was isolated as previously described (Parrett et al., 1989). The iron−sulfur clusters were reinserted into free PsaC-C14D according to a modification of a published procedure (Yu et al., 1993). Purified apoproteins were added to a final concentration of 0.5 mg mL^{-1} to a solution of 50 mM Tris-HCl (pH 8.3) containing 1% (w/w) β-mercaptoethanol. After 5 min of stirring at room temperature, a solution of 30 mM Na_2S was added slowly to a final concentration of 0.15 mM. After an additional 5 min of stirring at room temperature, a solution of 30 mM $FeCl_3$ was added slowly to a final concentration of 0.15 mM. The reaction mixture was incubated at 4 °C for 12 h. Excess inorganic reagents were removed from the reconstituted iron−sulfur proteins by gel filtration over Sephadex G-25 in an anaerobic chamber (Coy Laboratory Product Inc., Grass Lake, MI) and concentrated by centrifugation in a Centriprep device (Amicon Inc., Beverly, MA) under anaerobic conditions to a final protein concentration of 20 mg mL^{-1}. Rebinding of wild-type and mutant PsaC proteins on P700-F_X cores was accomplished as described previously (Parrett et al., 1990; Mehari et al., 1991; Li et al., 1991) except that the reconstituted PS I complex was purified of inorganic reagents and unbound PsaC and PsaD proteins by gel exclusion chromatography over Sephadex G-75 under anaerobic conditions. Protein concentrations were determined using a dye binding method (Bradford, 1976), and N-terminal amino acid sequencing of the overproduced PsaC-C14D mutant protein was performed with a Milligen/Biosearch 6600 ProSequencer at the University of Nebraska Protein Core Facility (Li et al., 1991).

Molecular Biology Protocols. The PsaC-C14D mutant protein was produced from a derivative of the pET expression plasmid pET36C which contains the *psaC* gene isolated from *Synechococcus* sp. strain PCC 7002 (Li et al., 1991). Site-directed mutagenesis was performed as previously described (Zhao et al., 1992; Kunkel et al., 1987). *Escherichia coli* strains harboring pET-36C (mutant *psaC*) were grown in medium NYZCM (Sambrook et al., 1989) except that magnesium sulfate was omitted. *Nostoc* sp. strain PCC 8009 PsaD (Li et al., 1991) was purified from solubilized inclusion bodies by chromatography on CM-Sepharose CL-6B with a linear gradient of sodium chloride (50−1000 mM). *Synechococcus* sp. strain PCC 7002 PsaE (Zhao et al., 1993) was purified from solubilized inclusion bodies by chromatography on DEAE-Sepharose CL 6B with a linear gradient of sodium chloride (10−200 mM) at pH 8.0.

Electron Paramagnetic Resonance Spectroscopy. Electron paramagnetic resonance (EPR) studies were performed with a Bruker ECS-106 X-band spectrometer equipped using either a standard-mode resonator (ER/4102 ST) or a bimodal resonator (ER 4116 DM). Mode changes were accomplished by tuning the microwave frequency to either ~9.6 GHz (parallel mode) or ~9.3 GHz (perpendicular mode). Spin quantitations were determined using a copper standard at a power level at least 1 order of magnitude below the $P_{1/2}$. Simulations of the EPR spectra were performed using "Qpow" (Belford & Belford, 1973; Belford & Nilges 1979) after recompiling the source code in Fortran 77SDK (Absoft, Rochester Hills, MI) to run on a Motorola 601 RISC microprocessor. All spectra were analyzed and plotted on a Power Macintosh 7100/80 computer using IgorPro 2.01 software (Wavemetrics, Lake Oswego, OR). Electrochemical redox titrations were performed in a specially-constructed EPR cell as described previously (Yu et al., 1993). The midpoint potential, E_m, was determined by least-squares-fitting to a linearized form of the Nernst equation: $E = E_m + (0.059/n)[\log([ox]/[red])]$.

Room Temperature Optical Studies. Flash-induced absorbance changes were measured in cooperation with Klaus Brettel at CEA-Saclay in a manner similar to that described in Bottin et al. (1987). The apparatus consisted of an 811 nm measuring beam provided by a collimated CW laser diode and a silicon photodetector. The output of the photodiode was amplified with an AM502 (Tektronix; gain of 100; DC to 1 MHz) and recorded with a DSA 602A digital oscilloscope (11A52 plug-in). Excitation was provided by two simultaneously fired xenon flashes; the duration of the flash was 3 μs. The optical path length for the measuring light was 1 cm. The PS I complexes were incubated with 100 μM phenazine methosulfate (PMS) and approximately 3 mg mL^{-1} sodium dithionite for 7 s in the dark, and the absorbance changes were measured in a three-flash sequence separated by 100 ms. The concentration of PMS was chosen to assure rereduction of $P700^+$ prior to recombination with F_A^- and or F_B^-. Sodium dithionite was used to reduce the PMS completely in order that oxidized PMS would not function as an electron accceptor.

Rates of $NADP^+$ Photoreduction. Rates of $NADP^+$ photoreduction mediated by flavodoxin and ferredoxin were measured in a 1.3 mL volume using reconstituted PS I complexes at 5 μg of Chl mL^{-1} in 50 mM Tricine, pH 8.0, 50 mM $MgCl_2$, 15 μM cytochrome c_6, 6 mM sodium ascorbate, and 0.05% dodecyl maltoside. P700-F_X cores from *Synechocystis* sp. strain PCC 6803 (Yu et al., 1995) were used instead of urea-isolated cores because the PsaC-minus strain sustained high rates of $NADP^+$ photoreduction when reconstitued with wild-type PsaC. Rates of flavodoxin-mediated $NADP^+$ photoreduction were measured with the

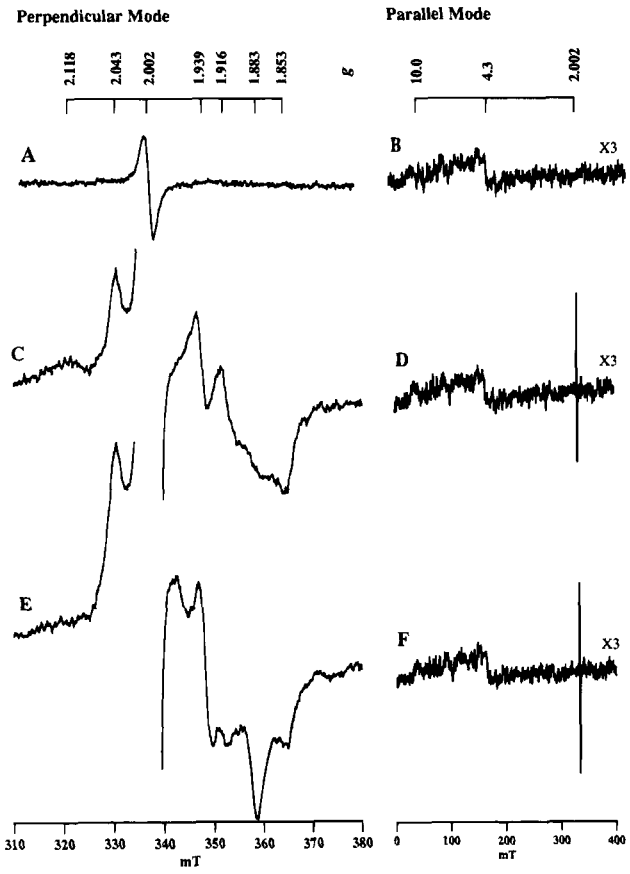

FIGURE 1: EPR spectra of the PS I complex reconstituted with PsaC-C14D under different conditions of illumination. Spectra on the left (A, C, and E) are recorded with the EPR resonator tuned to the perpendicular mode; spectra on the right (B, D, and F) are recorded with the resonator tuned to the parallel mode. The conditions are (A, B) freezing in darkness, (C, D) illumination at 15 K *minus* freezing in darkness, and (E, F) freezing during continuous illumination *minus* freezing in darkness. The large resonance near 345 mT in (C) and (E) is the photochemically-generated $P700^+$ radical at $g = 2.002$; this region was excised for clarity. The 250 μL sample contained 1 mg mL^{-1} Chl, 300 μM DCPIP, and 1 mM sodium ascorbate in 50 mM Tris buffer, pH 8.3, containing 0.04% Triton X-100. Spectrometer conditions: temperature, 15 K; microwave power, 20 mW; microwave frequency, 9.64591 GHz (perpendicular mode), 9.34542 GHz (parallel mode); modulation amplitude, 10 G at 100 kHz. The parallel-mode signal was expanded 3-fold in software.

addition of 0.5 mM $NADP^+$, 0.8 μM spinach ferredoxin: $NADP^+$ oxidoreductase (FNR; Sigma Chemical Co., St. Louis, MO), 0.1% β-mecaptoethanol, and 10 mM $MgCl_2$. Rates of ferredoxin-mediated $NADP^+$ photoreduction were measured under the same conditions except for the substitution of 5 μM *Synechococcus* sp. strain PCC 7002 ferredoxin for the 15 μM flavodoxin. Both measurements were made by monitoring the rate of change in the absorption of NADPH at 340 nm using a Cary 219 spectrophotometer fitted with appropriate narrow band and interference filters on the surface of the photomultiplier. The four-sided (clear) cuvette was illuminated from the both sides using two banks of high-intensity, red light-emitting diodes (LS1, Hansatech Ltd., Norfolk, U.K.).

RESULTS

EPR Spectral Properties of the Rebuilt PsaC-C14D−PS I Complex. Figure 1 shows EPR spectra of the rebuilt PsaC-C14D−PS I complex under different illumination regimes. In contrast to an earlier report (Zhao et al., 1992), there are no signals present in the dark around $g = 2.02$ (Figure 1A) that would indicate the presence of an oxidized [3Fe-4S] cluster (the minor resonance at $g = 2.002$ is due to an organic radical). When the solution potential is poised at +400 mV, no additional resonances are observed in this region. There are also no signals present around $g = 10$ that would indicate the presence of a reduced [3Fe-4S] cluster (a $[3Fe\text{-}4S]^0$ cluster is a paramagnetic $S = 2$ spin system). When the solution potential is poised at −650 mV, no additional resonances are observed in this region (data not shown). There was also little evidence for a reduced [3Fe-4S] cluster near $g = 10$ to 12 (Figure 1B) when the sample was examined by parallel-mode EPR spectroscopy, a method that is selective for integer spin systems. In contrast, the free PsaC-C14D protein shows an intense derivative signal in the parallel mode at $g = 11.5$ derived from the $S = 2$, $[3Fe\text{-}4S]^0$ cluster (see Figure 7). One difference between the two experiments is that the sample in this study was rigorously shielded from light. The sharp resonances around $g = 2$ in Zhao et al. (1992) may have been derived from an organic radical, perhaps a cysteine sulfhydryl, generated from the strong reductants available on illumination. Another difference is that the PsaC-C14D protein in this study was purified of inorganic reagents by anaerobic gel filtration chromatography prior to rebinding onto P700-F_X cores.

When the PsaC-C14D−PS I complex is frozen in darkness and illuminated at 15 K, a strong set of resonances are present at $g = 2.043$, 1.939, and 1.853 characteristic of F_A (Figure 1C). There is a second spin system present with *apparent* g-values of 2.118, 1.916, and 1.883 and broader line widths. These resonances were detected in our previous study (Zhao et al., 1992), but because of the interfering dark resonances, it was not clear whether they represented a second spin system or an artifact. This signal, termed F_B', is most likely a [4Fe-4S] cluster located in the aspartate-modified site. As shown in Figure 1D, this $S = {}^1/_2$ spin system is not observed in the parallel mode, and there is only a hint of a resonance at $g = 10$ to 12 that could be attributed to a reduced $[3Fe\text{-}4S]^0$ cluster (the derivative-shaped line at 330 mT is due to the intense $P700^+$ radical visible because of mechanical imperfections in the dual-mode cavity). When the PsaC-C14D−PS I complex is photoaccumulated by freezing under illumination, the spectrum changes (Figure 1E): the F_B' resonance at $g = 2.118$ and the F_A resonance at $g = 1.853$ diminish in intensity, and the resonances at $g = 2.043$, 1.939, and 1.883 increase in intensity. This behavior is similar to that of F_A and F_B in a wild-type PS I complex, where magnetic coupling between the two clusters leads to an interaction-type spectrum. The spin concentration in Figure 1E is equal to a sample that has been prereduced with sodium dithionite in darkness at pH 10.5 (not shown), indicating nearly quantitative reduction of the iron−sulfur clusters with light. The minor resonances at $g = 1.916$ and 1.853 in Figure 1E may be due to F_B' and F_A that are not spin-coupled. No additional resonances are observed in the parallel mode under highly reducing conditions (Figure 1F). These results show that the $[3Fe\text{-}4S]^{1+,0}$ cluster, that is clearly present in free PsaC-C14D, is not a component of the PS I complexes reconstituted with PsaC-C14D, and that a second spin system is present which is most likely a mixed-ligand [4Fe-4S] cluster in the F_B site.

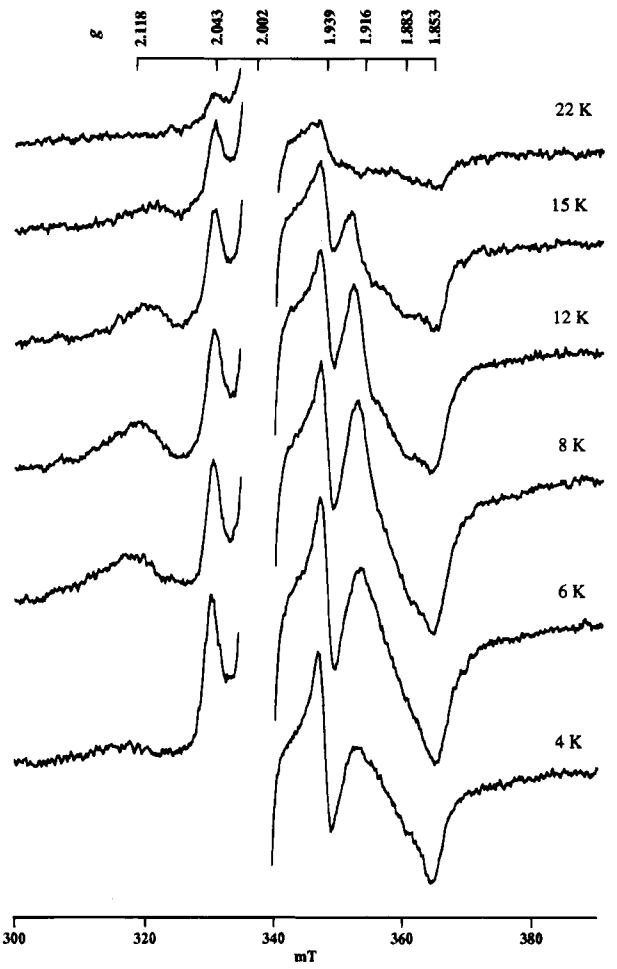

FIGURE 2: Temperature dependence of the EPR resonances in a PS I complex reconstituted with PsaC-C14D frozen in darkness and illuminated at 10 K. The 250 μL sample contained 1 mg mL^{-1} Chl, 300 μM DCPIP, and 1 mM sodium ascorbate in 50 mM Tris buffer, pH 8.3. The region surrounding 335 mT was excised for clarity; it contained only the large derivative-shaped signal from the P700$^+$ radical at $g = 2.002$. Spectrometer conditions: microwave power, 20 mW; microwave frequency, 9.448 GHz; modulation amplitude, 10 G at 100 kHz.

Temperature Dependence of F_A and F_B'. The temperature dependence of the photoaccumulated spectrum in the rebuilt PsaC-C14D−PS I complex is shown in Figure 2. The F_A resonances at $g = 2.043$, 1.939, and 1.853 increase steadily in intensity as the temperature is lowered from 22 to 4.2 K. This signal does not behave identically to F_A in a wild-type PS I complex, for which the spin relaxation process results in a maximum signal intensity at 15 K. The F_B' resonances at *apparent* g-values of 2.118, 1.916, and 1.883 increase in intensity as the temperature is lowered from 22 K and attain a maximum intensity at 8 K. The signals then decrease in intensity to 4.2 K, and at the lowest temperatures, microwave power saturation has rendered F_B' nearly undetectable. The different spin relaxation rates of F_B' and F_A are responsible for the change in the shape of the overall spectrum throughout this temperature range. One consequence is that the spectral features of the F_A cluster can be extracted at very low temperatures. Except for a slight low-field shoulder on the $g = 1.853$ resonance, the g-values of this spin system are consistent with its identification as F_A. The altered relaxation behavior of F_A in the PsaC-C14D−PS I complex relative to wild-type PS I complexes shows that the modified structure of the F_B' site leads to subtle changes that can be transmitted to the F_A site.

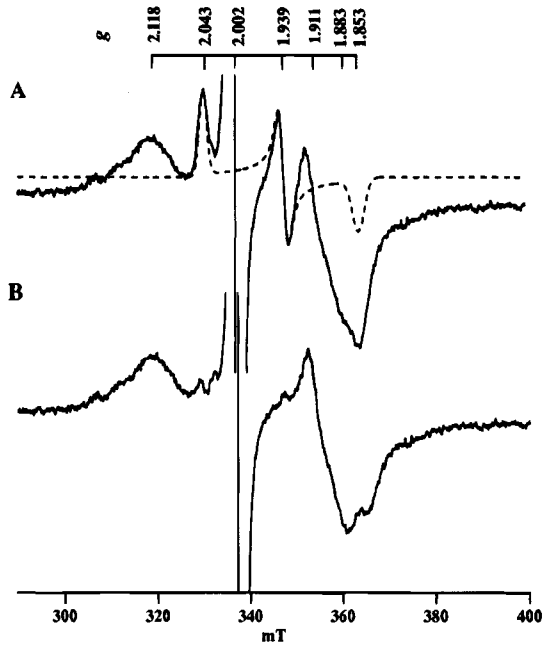

FIGURE 3: Spectral features of the F_B' cluster in a PS I complex reconstituted with PsaC-C14D. The solid line in (A) represents the spectrum of a sample which was frozen in darkness and illuminated at 8 K. The dotted line represents the simulated spectrum of F_A, with g-values of 2.043, 1.939, and 1.853 and line widths of 30, 28.5, and 40 MHz, respectively. The region surrounding 335 mT was excised for clarity; it contained only the large derivative-shaped signal from the P700$^+$ radical at $g = 2.002$. The spectrum in (B) represents that of F_B' with the F_A resonances subtracted. The 250 μL sample contained 1 mg mL^{-1} Chl, 300 μM DCPIP, and 1 mM sodium ascorbate in 50 mM Tris buffer, pH 8.3. Conditions for simulation of the F_A spectrum are provided under Materials and Methods. Spectrometer conditions: temperature, 8 K; microwave power, 20 mW; microwave frequency, 9.448 GHz; modulation amplitude, 10 G at 100 kHz.

EPR Spectral Features of F_B'. The spectral features of F_B' are extracted by subtracting the spectrum of F_A from the composite spectrum under conditions where only one electron is transferred from P700. Figure 3A shows a spectral simulation of F_A (dashed line) along with the composite spectrum of the PsaC-C14D−PS I complex after illumination at 8 K (solid line). The simulation of F_A was carried out assuming g-values of 2.043, 1.939, and 1.853 and line widths of 30, 28.5, and 40 MHz; however, the problem of g-strain broadening in iron−sulfur proteins may result in a skewing of the high-field trough and low-field peak and an asymmetry of the derivative midfield feature. As shown in Figure 3B, the F_B' g-values of 2.118, 1.911, and 1.883 and the broader line widths are significantly different from F_B in a wild-type PS I complex. The half-saturation parameters for F_B' and F_A were determined at a variety of temperatures. When measured at 12 K, the $P_{1/2}$ value for the $g = 2.118$ resonance of F_B' was $\geq$200 mW, and the $P_{1/2}$ values for the $g = 2.043$ and 1.939 resonances of F_A were 55 and 50 mW, respectively (data not shown). The latter $P_{1/2}$ values are compatible with the proposal that these two signals are derived from the F_A cluster. In contrast, the $P_{1/2}$ values for the $g = 2.043$ and 1.939 lines of F_A in the wild-type PS I complex are about 5 mW when measured at 12 K. These data show that the spin relaxation rates of both the F_A and F_B' clusters have been altered by the aspartate mutation in position 14 of PsaC.

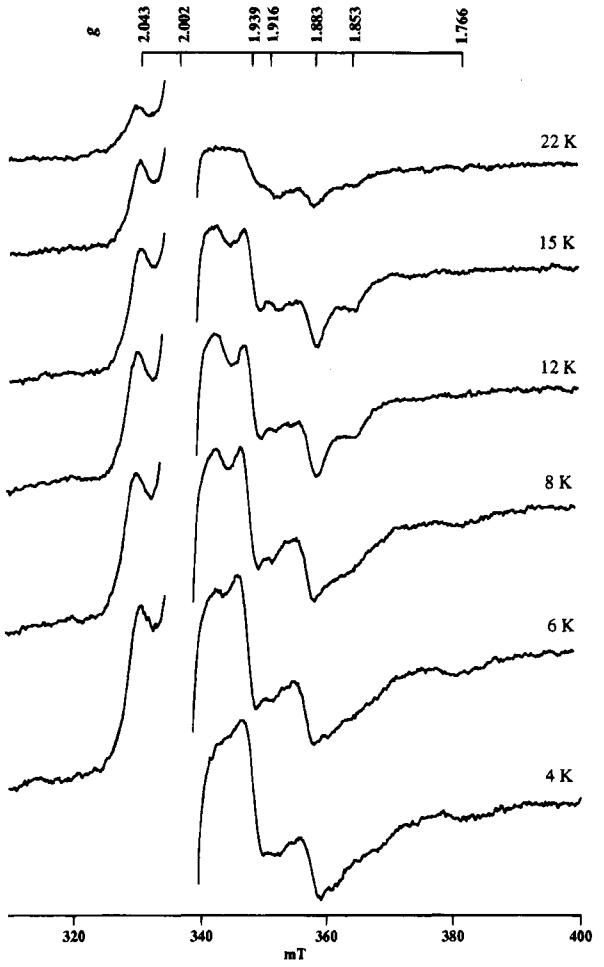

FIGURE 4: Temperature dependence of the EPR resonances in a PS I complex reconstituted with PsaC-C14D under conditions where the sample was illuminated during freezing. The region surrounding 335 mT was excised for clarity; it contained only the large derivative-shaped signal from the $P700^+$ radical at $g = 2.002$. The 250 μL sample contained 1 mg mL^{-1} Chl, 300 μM DCPIP, and 1 mM sodium ascorbate in 50 mM Tris buffer, pH 8.3. Spectrometer conditions: microwave power, 20 mW; microwave frequency, 9.448 GHz; modulation amplitude, 10 G at 100 kHz.

Temperature Dependence of Photoaccumulated F_A and F_B'. Figure 4 illustrates the temperature dependence of the EPR spectrum under conditions where F_A and F_B' have been photoaccumulated. Unlike a wild-type PS I complex, for which the signals are maximum at 15−18 K, the resonances at $g = 2.043$ and 1.939 in the PsaC-C14D−PS I complex increase in intensity as the temperature is lowered to 4.2 K. The appearance of the spectrum at field positions above 360 mT changes as the temperature is lowered, with the high-field side of the interaction signal at $g = 1.883$ developing a distinct shoulder. This signal is derived from F_A under conditions where the second spin system is either not present or not reduced. Since the rapid relaxation properties of the F_A cluster lead to a spectrum with maximum intensity at 4.2 K, the high-field shoulder at 365 mT can be rationalized as a superposition of an increased contribution of F_A relative to the interaction spectrum. The resonance at $g = 1.766$ indicates that some F_X also becomes photoreduced under these experimental conditions. The high-field shoulder of the interaction spectrum around 365 mT will therefore contain a small contribution from the $g = 1.86$ midfield resonance of F_X.

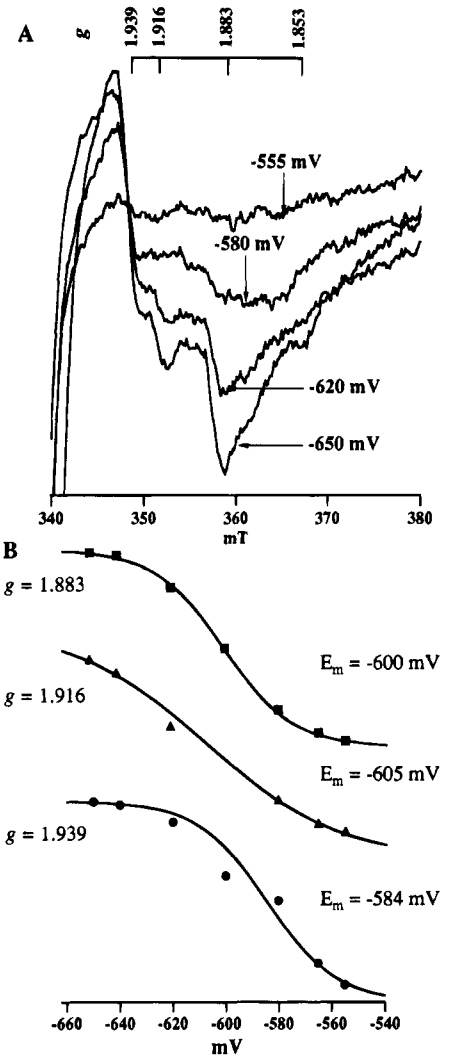

FIGURE 5: Redox titration of the PS I complex reconstituted with PsaC-C14D at 4 K. The spectra in (A) show the interaction spectrum from reduced F_A and F_B' in the region between 340 and 380 mT. The Nerstian fit of the intensity of the resonances as a function of imposed potential is shown in (B) for the $g = 1.883$ resonance (top), the 1.916 resonance (middle), and the 1.939 resonance (bottom). The E_m and n-values are calculated by the best-fit to the data. The 400 μL sample contained 1.2 mg mL^{-1} Chl, 0.5 mM 4,4′-dimethyl-*N*,*N*′-trimethylene-2.2′-dipyridinium dibromide, 0.5 mM *N*,*N*′-trimethylene-2,2′-dipyridinium dibromide, and 0.5 mM 1,1′-dimethyl-4,4′-bipyridinium dichloride in 50 mM glycine buffer, pH 10.0. Spectrometer conditions: microwave power, 20 mW; microwave frequency, 9.448 GHz; modulation amplitude, 10 G at 100 kHz. The sample was kept in total darkness throughout the entire procedure. The temperature was 4.2 K.

Reduction Potentials of F_A and F_B'. The midpoint potentials of F_A and F_B' in PsaC-C14D−PS I were determined electrochemically by redox poising the sample in the dark and using EPR detection at 4.2 K. As shown in Figure 5A, neither F_A nor F_B' is visible when the solution is poised at a potential of −555 mV. As the solution potential is lowered to −580 mV, the spectral features begin to develop, and by −620 mV, the resonances have already taken the appearance of the interaction spectrum described in Figure 4. At −650 mV, the spectrum is fully developed and is not substantially different from that at −620 mV except for intensity. The end point of the titration was reached by thawing the −650 mV sample and refreezing under continuous illumination; except for the appearance of features due to reduction of F_X, the spectrum of the interaction signal

was unchanged. A plot of the signal intensity versus potential for the resonances at $g = 1.883$ (top), 1.916 (middle), and 1.939 (bottom) is shown in Figure 5B. Since the EPR resonances at imposed potentials less than −580 mV show an interaction spectrum, the F_A and F_B clusters have similar midpoint potentials. The $g = 1.939$ midfield line of the interaction spectrum titrates with a Nernstian response at a midpoint potential of −584 mV and an n value of 1.95. Similarly, the $g = 1.883$ high-field trough titrates with a midpoint potential of −605 mV, and an n value of 2.00. The n value of 2 implies that these two lines represent a spectrum contributed by two spin systems, similar to the two-electron changes that were found in the titration of the $g = 2.05$, 1.94, and 1.89 lines of the wild-type PS I complexes (Ke et al., 1973). Since F_B titrates with a midpoint potential of −580 mV in wild-type PS I, the midpoint potential of −600 mV indicates that the cysteine to aspartate change has a minor effect on F_B'. There is a greater effect on the distant, unmodified F_A site. F_A titrates with an E_m of −520 mV in wild-type PS I (Ke et al., 1973); hence, the reduction potential of F_A in the PsaC-C14D−PS I complex has been driven 80 mV more reducing due to the mutation in the F_B site. The $g = 1.916$ line, which is suspected to arise from F_B' clusters which are not magnetically interacting with F_A, titrates with a midpoint potential of −605 mV and an n value of 1.02.

Optical Studies of F_A and F_B' at Room Temperature. The number of electron acceptors functioning subsequent to F_X can be determined at room temperature by the number of electrons that can be stabilized for more than 1 ms during a series of saturating flashes (Sauer et al., 1978). As shown in Figure 6A, the reduction of $P700^+$ in a wild-type PS I complex occurs with a $t_{1/2}$ of 2.0 ms on the first flash and 1.85 ms on the second flash, followed by a dominant phase with $t_{1/2}$ of ~200 μs on the third flash. The millisecond kinetics represent the half-time of the electron transfer from PMS to $P700^+$, accounting for >90% of the absorbance change, and the microsecond kinetics represent the $P700^+$ F_X^- back-reaction, accounting for 55% of the total absorbance change (the remainder is represented by a slower decay that was not characterized). In the PsaC-C14D−PS I complex (Figure 6B), the reduction of $P700^+$ occurred with $t_{1/2}$ of 1.5 ms on the first flash and 0.90 ms on the second flash, followed by a dominant phase with a $t_{1/2}$ of ~300 μs on the third flash. The millisecond kinetics represent primarily the half-time of electron transfer from PMS to $P700^+$, but there is also a small contribution (about 15%) of a ~200 μs kinetic phase. This may be due to the $P700^+$ F_X^- back-reaction that results from inefficient forward electron transfer or from a population of nonreconstituted P700-F_X cores. The kinetics on the third flash are due to the $P700^+$ F_X^- back-reaction and account for 70% of the total absorbance change. Thus, two electron acceptors function subsequent to F_X in a PsaC-C14D−PS I complex, consistent with the ability of F_A and F_B' to accept an electron efficiently at room temperature.

As shown in Table 1, rates of $NADP^+$ photoreduction in the PsaC-C14D−PS I complex are about 70% that of a reconstituted PsaC−PS I complex. The rates are identical whether ferredoxin or flavodoxin functions as the electron acceptor. The implication is that electron throughput from F_X to soluble electron carriers is influenced by the presence of the mixed-ligand [4Fe-4S] cluster in the F_B' site, or the altered reduction potential of F_A. Either inefficient reconstitution of PsaC-C14D onto P700-F_X cores or inefficient forward electron transfer from F_X is the reason behind the lower rates. Either mechanism is consistent with Figure 4, where a population of photoreduced F_X can be observed in the rebound PsaC-C14D−PS I complex.

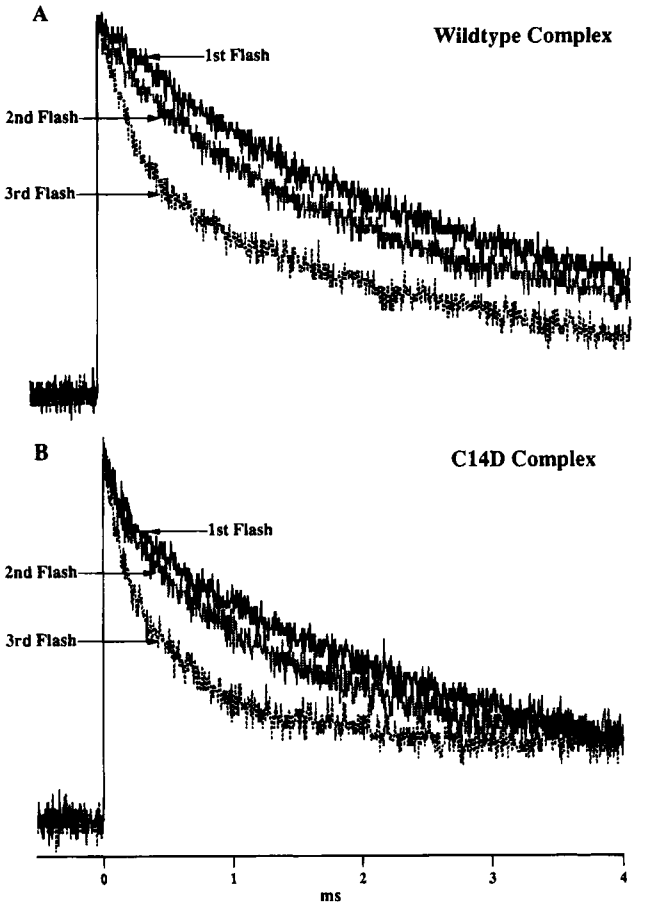

FIGURE 6: Time course of flash-induced absorption changes at 811 nm in (A) wild-type PSI complexes and (B) PS I complexes reconstituted with PsaC-C14D. The complexes were incubated with 100 μM PMS and approximately 3 mg mL^{-1} sodium dithionite for 7 s in the dark prior to the onset of the flash train. The flashes were separated by 100 ms. The absorbance changes are depicted for the first, second, and third flashes, respectively. The data show the result of a single measurement. The absorbance changes were normalized to the first flash; in practice, only minor corrections were necessary (the maximum correction was 15%).

Table 1: $NADP^+$ Photoreduction Rates

sample	$NADP^+$ reduction[a]	
	flavodoxin	ferredoxin
wild-type PS I	305	342
PsaC-less[b]	70	38
PsaC−PS I[c]	312	300
PsaC-C14D−PS I[c]	220	211

[a] Rates in micromoles per milligrams of chlorophyll per hour. [b] The PsaC-less mutant is *Synechocystis* sp. strain PCC 6803 (missing PsaC, PsaD, and PsaE). [c] Reconstituted with *Nostoc* sp. strain PCC 8009 PsaD and *Synechococcus* sp. strain PCC 7002 PsaE.

Origin of the [4Fe-4S] Cluster in the Modified PsaC-C14D Mutant Site. The F_B' cluster in the rebuilt PsaC-C14D−PS I complex may be derived from a population of mixed-ligand [4Fe-4S] clusters in the free PsaC-C14D protein. The spectral region between 300 and 400 mT shows distorted resonances due to saturation of the $S = 1/2$, $[4Fe\text{-}4S]^{1+}$ cluster in the unmodified F_A site, and in the region between 0 and

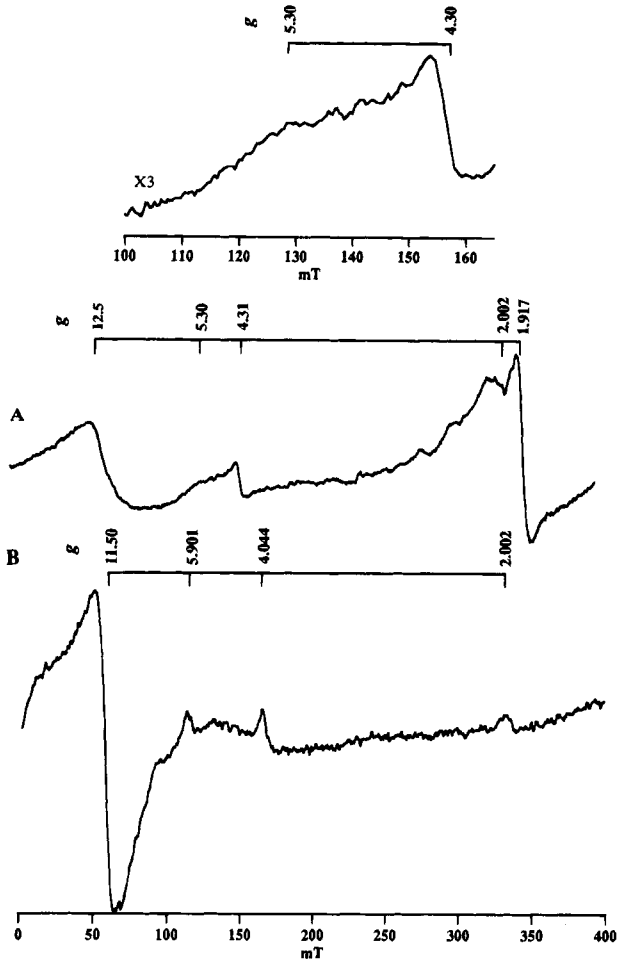

FIGURE 7: Spectrum of the iron–sulfur clusters in the unbound PsaC-C14D protein in (A) the perpendicular mode and (B) the parallel mode. The S = 2, $[3Fe\text{-}4S]^0$ cluster and the $S = {}^1/_2$, $[4Fe\text{-}4S]^{1+}$ cluster are both observed in the perpendicular mode after addition of sodium dithionite at pH 10. Only the $S = 2$, $[3Fe\text{-}4S]^0$ cluster is seen in the parallel mode at $g = 11.50$ (defined as the middle of the derivative-shaped resonance). The inset above (A) contains the region between 100 and 180 mT after vertical expansion of the perpendicular mode spectrum by a factor of 3. Spectrometer conditions: dual mode resonator: microwave power, 80 mW; microwave frequency, 9.6431 GHz (perpendicular mode), 9.3369 GHz (parallel mode); modulation amplitude, 10 G at 100 kHz; temperature, 4.2 K.

100 mT, a broad resonance derived from the reduced $[3Fe\text{-}4S]^0$ cluster in the modified F_B site (Figure 7A). This single asymmetric feature has all of the characteristics of a reduced [3Fe-4S] cluster, including the line shape which tails toward the low field, with broadening into zero field. The intensity of the parallel-mode EPR spectrum increases by a factor of 2.5, and the resonances due to the reduced [4Fe-4S] cluster disappear, behavior which is expected under the selection rules for $S = 2$ and $S = {}^1/_2$ spin systems. This shows that the $[3Fe\text{-}4S]^{0,1+}$ cluster in free PsaC-C14D remains intact when the unmodified $[4Fe\text{-}4S]^{1+,2+}$ cluster is reduced.

The strong asymmetric resonance at $g = 4.30$ is due to the presence of a high-spin ($S = {}^5/_2$) d^5 Fe^{3+} ion in an octahedral environment (Figure 7A). It is probably derived from adventitious iron carried over from the iron–sulfur center reconstitution protocol and located in an environment inaccessible to dithionite. Just downfield is a broad peak between 100 and 160 mT (Figure 7, inset) which has relaxation properties different from the resonance at $g = 4.3$. This $g = 5.3$ resonance(s) can only be observed at very low temperatures and high microwave powers, consistent with its identification as one or two unresolved low-field resonances from a high-spin [4Fe-4S] cluster. Assuming a spin state of $S = {}^3/_2$ and an *E/D* value of 0.3, the two Kramers doublets would result in low-field resonances at $g_{eff} = 5.37$ and 5.55 (it is not certain whether just the lower or both the higher and lower energy doublets are present). While the intensity of the $g = 5.3$ line(s) appears to be small, the anisotropy of the g-tensor for a $S = {}^3/_2$ spin system is distributed well over 350 mT in the rhombic limit. Hence, the low-field turning point feature will appear small when the resonance is depicted as a (pseudo) first-derivative signal. This problem is inherent in the low intensity of highly anisotropic spectra from high-spin systems.

DISCUSSION

The rationale behind these experiments was to provide a detailed characterization of the types and properties of iron–sulfur clusters in a reconstituted PsaC-C14D–PS I complex. Although an exhaustive search was performed, no evidence for the presence of a $[3Fe\text{-}4S]^{1+,0}$ cluster could be found, even though the $[3Fe\text{-}4S]^{1+,0}$ cluster clearly exists in the free PsaC-C14D protein. Instead, a second spin system was identified in the PsaC-C14D–PS I complex, and the g_{av} of 1.97 unambiguously identifies this signal as derived from an iron–sulfur cluster. Since the F_A cluster is assigned to the unmodified site by virtue of its g-values and response to light at 15 K, the second spin system is identified, by default, as a modified F_B' in the mixed-ligand site. It seems highly likely that F_B' is a [4Fe-4S] cluster, since a 1Fe, rubredoxin-like center would be expected to remain in a spin state of $S = {}^5/_2$ due to the relatively weak tetrahedral field of the four cysteine ligands, and there is no precedent for the insertion of a [2Fe-2S] cluster into a [4Fe-4S] protein.

The modified F_B' cluster has *apparent* g-values of 2.118, 1.916, and 1.883 and line widths on the order of 100 MHz, resulting in a merging of the the midfield and high-field resonances. On reduction of both clusters, the $g = 2.118$ low-field resonance of F_B' and the $g = 1.853$ high-field resonance of F_A disappear, and a spectrum appears characteristic of magnetically-interacting centers. The midpoint potential of ca. −600 mV is only 20 mV lower than F_B in the wild-type complex, implying that an aspartate in the cysteine site does not significantly change the redox character of this cluster. The relative spin relaxation rates of both F_A and F_B', inferred from the temperature dependence and half-saturation parameter, are more rapid than those of F_A and F_B in the wild-type complex. The EPR and optical kinetic data indicate that F_A and F_B' are capable of accepting an electron at cryogenic and room temperatures. Single-turnover flash experiments show that both clusters function as efficient electron acceptors. The rates of $NADP^+$ photoreduction indicate that electron throughput is diminished by 30% relative to wild-type rates. One major difference from the wild-type PS I complex is that a larger amount of F_B' is photoreduced at temperatures of 8–15 K in PsaC-C14D–PS I than is F_B in a wild-type PS I complex. The similar equal midpoint potentials of F_A and F_B' may play a role in allowing both electron acceptors to be available for photoreduction at low temperatures.

Assuming a mixed-ligand, [4Fe-4S] cluster exists in PsaC-C14D–PS I complexes, it is reasonable to consider the origin

of this cluster, since it was previously shown that PsaC-C14D−PS I contains a [3Fe-4S] cluster in the F_B site (Yu et al., 1993). In the extension of those studies, evidence is presented here for the the existence of a $S = {}^3/_2$, [4Fe-4S] cluster in free PsaC-C14D. One likely possibility is that the P700-F_X core preferentially binds those PsaC-C14D proteins that contain two [4Fe-4S] clusters rather than PsaC-C14D proteins containing one [3Fe-4S] and one [4Fe-4S] cluster. This is consistent with the finding that a 10-fold higher concentration of PsaC-C14D than wild-type PsaC is required in the reconstitution protocol. The binding requirements for PsaC must be stringent, at least in an *in vitro* reconstitution protocol, since the binding minimally appears to have a requirement for two intact [4Fe-4S] clusters and a well-preserved three-dimensional structure for the PsaC protein. A dynamic process could also be envisioned in which there is an equilibrium between the [3Fe-4S] and [4Fe-4S] forms of the protein, as some iron is probably available for such an interconversion.

If the population of PsaC-C14D proteins containing $S = {}^3/_2$, [4Fe-4S] clusters are selectively bound by the P700-F_X core during reconstitution, the mixed-ligand [4Fe-4S] cluster must cross over from a $S = {}^3/_2$ spin state to a $S = {}^1/_2$ spin state upon binding to the P700-F_X core. The crossover energies are likely to be very small. An example is provided by the *Azotobacter vinelandii* Fe protein, that exists in a mixture of interconvertible $S = {}^1/_2$ and $S = {}^3/_2$ spin states. The addition of 2 M urea causes the spin states to become predominantly $S = {}^3/_2$, and addition of 80% ethylene glycol causes the spin states to become predominantly $S = {}^1/_2$ (Lindahl et al., 1985). Unlike the change to aspartate, that affects the inner coordination sphere of the iron−sulfur cluster, solvent effects clearly operate at the outer coordination sphere. If a change in the solvent is sufficient to influence the spin state of the *A. vinelandii* Fe protein, then it does not seem unreasonable to propose that the binding of PsaC, PsaD, and PsaE to the P700-F_X core induces changes that might similarly influence the strength of the crystal field splittings. This could allow the crossover energy to be exceeded, thereby favoring the $S = {}^1/_2$ spin state of the [4Fe-4S] cluster in the modified site.

In summary, evidence is provided that a PsaC protein harboring a mixed-ligand F_B' cluster can be functionally rebound to the PS I complex. The altered cluster affects the spin-relaxation properties and redox potentials of both the F_A and F_B' clusters. Although the midpoint potential of the F_A cluster is shifted approximately 80 mV more reducing than in wild-type PsaC, electron transport to F_A and F_B' appears to occur efficiently, and rates of $NADP^+$ photoreduction are 70% that of a PS I complex rebuilt with wild-type PsaC. These results also show that a mixed-ligand [4Fe-4S] cluster is capable of participating as an electron transfer agent in a physiologically-relevant setting, i.e., within a functional PS I complex, a property that is difficult to demonstrate with soluble ferredoxins that have undefined roles in electron transfer in cellular metabolism.

ACKNOWLEDGMENT

We thank Dr. Klaus Brettel, Section de Bioénergétique, CEA-Saclay, 91191 Gif-sur-Yvette Cedex, France, for performing the measurement of the room temperature, flash-induced absorbance changes at 811 nm; Dr. Fred Hawkridge, Virginia Commonwealth University, for the generous gift of *N,N'*-trimethylene-2,2'-dipyridinium dibromide; and Dr. Michael Johnson for many stimulating and fruitful discussions concerning the properties of high-spin iron−sulfur clusters.

REFERENCES

Belford, R. L., & Belford, G. G. (1973) *J. Chem. Phys. 59,* 853−854.

Belford, R. L., & Nilges, M. J. (1979) EPR Symposium, 21st Rocky Mountain Conference, Denver, CO, Aug 1979.

Bottin, H., Sétif, P., & Mathis, P. (1987) *Biochim. Biophys. Acta 894,* 39−48.

Bradford, M. M. (1976) *Anal. Biochem. 72,* 248−254.

Fromme, P., Schubert, W. D., & Krauss, N. (1994) *Biochim. Biophys. Acta 1187,* 99−105.

Jensen, G. M., Warshel, A., & Stephens, P. J. (1994) *Biochemistry 33,* 10911−10924.

Ke, B., Hansen, R. E., & Beinert, H. (1973) *Proc. Natl. Acad. Sci. U.S.A. 70,* 2941−2945.

Krauss, N., Hinrichs, W., Witt, I., Fromme, P., Pritzkow, W., Dauter, Z., Betzel, C., Wilson, K. S., Witt, H. T., & Saenger, W. (1993) *Nature 361,* 326−331.

Kunkel, T. A., Roberts, J. D., & Zabour, R. A. (1987) *Methods Enzymol. 154,* 367−382.

Langen, R., Jensen, G. M., Jacob, U., Stephens, P. J., & Warshel, A. (1992) *J. Biol. Chem. 267,* 25625−25627.

Li, N., Zhao, J., Warren, P. V., Warden, J., Bryant, D. A., & Golbeck, J. H. (1991) *Biochemistry 30,* 7863−7872.

Lindahl, P. A., Day, E. P., Kent, T. A., Orme-Johnson, W. H., & Münck, E. (1985) *J. Biol. Chem. 260,* 11160−11173.

Mehari, T., Parrett, K. G., Warren, P. V., & Golbeck, J. H. (1991) *Biochim. Biophys. Acta 1056,* 139−148.

Parrett, K. G., Mehari, T., Warren, P. G., & Golbeck, J. H. (1989) *Biochim. Biophys. Acta 973,* 324−332.

Parrett, K. G., Mehari, T., & Golbeck, J. H. (1990) *Biochim. Biophys. Acta 1015,* 341−352.

Sambrook, J., Fritsch, E. F., & Maniatis, T. (1989) *Molecular Cloning: A Laboratory Manual,* 2nd ed., Cold Spring Harbor Laboratory, Cold Spring Harbor, NY.

Sauer, K., Mathis, P., Acker, S., & Van Best, J. A. (1978) *Biochim. Biophys. Acta 503,* 120−134.

Yu, L., Zhao, J. D., Lu, W. P., Bryant, D. A., & Golbeck, J. H. (1993) *Biochemistry 32,* 8251−8258.

Yu, J., Smart, L. B., Jung, Y.-S., Golbeck, J. H., & McIntosh, L. (1995) *Plant Mol. Biol.* (in press).

Zhao, J., Li, N., Warren, P. V., Golbeck, J. H., & Bryant, D. A. (1992) *Biochemistry 31,* 5093−5099.

Zhao, J., Snyder, W. B., Mühlenhoff, U., Rhiel, E., Warren, P. V., Golbeck, J. H., & Bryant, D. A. (1993) *Mol. Microbiol. 9,* 183−194.

BI942755M